

Infrared Missile Domes: Is there a Figure of Merit for Thermal Shock?

Claude A. Klein

*Raytheon Company, Research Division
Lexington, Massachusetts 02173*

Abstract. Since most materials that possess favorable optical properties in the infrared (IR) are relatively weak brittle solids, the problem of selecting dome materials for advanced IR-guided or dual-mode missiles requires a careful assessment of the dome's ability to withstand the thermal shock induced by transient heating on a fly-out trajectory. In this regard, it has become common practice to rely on simple figures of merit such as the "parameters" R and R' [D. Hasselman, *Ceram. Bull.* **49**, 1033 (1970)] for ranking the predicted performance of IR dome material candidates. It is the purpose of this paper to demonstrate that the concept of a "universal" figure of merit for thermal shock has no merit since the ability of an IR dome to survive transient thermal stresses depends not only on intrinsic material properties but also on the thermal environment as characterized by the Biot number (Bi). For this reason, the thickness of the dome plays an essential role because it may have an impact on the heat-flow regime (thermally thick or thermally thin) and, therefore, on peak thermal stresses. Furthermore, in a thermally thin regime ($Bi < 1$), the resistance to thermal shock will be enhanced by making the dome as thin as possible, that is, as determined by structural requirements, which are not reflected in the derivation of the Hasselman parameters. The procedure outlined in this paper provides a direct measure of the thermal shock resistance (TSR) in the sense that it yields the "ultimate" thermal shock temperature, *i.e.*, the allowable recovery temperature rise above the wall temperature at the onset of the shock. For "thick" domes, the thermal shock should be essentially independent of the geometry and the environment; for "thin" domes, on the contrary, the performance depends not only on a specific material property combination, or figure of merit, but also on the radius of the dome and the aerodynamic/aerothermal load. In a first approximation, the TSR of a "thick" dome will be controlled by the figure of merit $R = \sigma_f(1-\nu)/(\alpha E)$, which is precisely the Hasselman parameter for high rates of convective heating, while in a thermally thin regime the appropriate figure of merit should be $\text{mod. } R' = \sigma_f^{5/3}(1-\nu)k/(\alpha E)$, which includes the thermal conductivity in the same manner as the Hasselman parameter R' for low rates of heat transfer but weighs the flexural strength more heavily. In order to illustrate the discussion, it is shown how IR dome material candidates can be ranked in terms of their ability to survive the thermal shock on a "most severe" air-to-air missile trajectory.

1. Introduction

The primary function of an infrared (IR) missile dome is to protect the guidance system against environmental "loads" originating from high-speed flight through the atmosphere, and this function must be carried out without seriously degrading the performance of the seeker. There are many reasons why IR transmitting materials may fail to perform properly in a missile-dome application. In this paper, we are concerned with the thermostructural capabilities of IR domes, that is, issues relating to failure as a result of dome fracture induced by thermal shock. Immediately after launch, a missile rapidly accelerates, which subjects the dome to intense heat loads stemming from forced convection caused by the rise in temperature of the air in immediate contact with the outer dome surface. The dome's thermal response then results in severe temperature gradients through the thickness, which in turn generates transient stresses that manifest themselves as a compression at the outer surface and a tension at the inner surface.¹ If this tensile stress exceeds the nominal strength of the dome material, catastrophic failure may occur; we will refer to this failure mode as thermal shock induced fracture, keeping in mind that, in a flight environment, failure may also occur simply because of elevated temperatures, but this is not a relevant consideration in the present context.

The flight velocities of future-generation missiles are projected to far exceed the performances of contemporary systems, which raises the issue of how to assess the thermostructural capability of IR dome material candidates. To do this properly, the thermal shock resistance (TSR) of each candidate must be evaluated in the appropriate dome geometry, which means finite-element analysis of the transient stress distributions coupled with fracture-statistical model calculations. This task, however, requires a complete set of data, or data base, that includes the thermal and mechanical properties of both, the IR transmitting material as well as the contemplated attachment structure, which may not be available, especially at temperatures of interest in a dynamic flight environment. For this reason, and in lieu of a comprehensive analysis, it has become common practice (see, for instance, Ref. 2) to rely on figures of merit (FoM) for ranking dome-material candidates in terms of their ability to withstand the thermal shock. The figures of merit that have been adopted are the two so-called "Hasselman parameters," R and R' , that characterize the TSR of a spherical ceramic monolith³; specifically,

$$R = \frac{\sigma_f (1-\nu)}{\alpha E} \quad (1)$$

for thermally "severe" situations and

$$R' = \frac{\sigma_f (1-\nu) k}{\alpha E} \quad (2)$$

under thermally "mild" conditions. Evidently, and this was emphasized by Kingery⁴ as early as 1955, the resistance to thermal shock cannot be considered an intrinsic material property because it depends on the manner in which the heat load is applied, and how the shape or geometry of the component affects the stress distribution.

* The notations are as specified in the Glossary.

In a missile-dome application, the thermal shock environment as defined by the Biot number,

$$Bi \equiv hL/k, \quad (3)$$

where h designates the heat-transfer coefficient at the outer surface, L is the dome thickness, and k refers to the thermal conductivity of the dome material, usually points to $Bi \approx 1$,² which suggests "intermediate" type conditions and, therefore, does not allow us to draw firm conclusions from simplistic FoMs such as R and R' . Furthermore, it is well-established (see, for instance, Ref. 5) that the thickness of the dome plays a critical role in the sense that the parameter L can have a major impact on the thermal stress, which is not reflected in the derivation of the expressions (1) and (2). In fact, even a cursory review of relevant literature leads to the conclusion that, because of the synergy of the process and the conflicting results of experimental testing, comparing or estimating the TSR of potential dome materials on the basis of material property combinations *à la* Hasselman does not give reliable indications and should indeed be treated with caution.⁶ It is also apparent that much of the literature on TSR capabilities of IR domes betrays a lack of proper understanding of the fundamentals that control the thermal stress situation. The purpose of this paper, therefore, is to consider the key aspects of the problem, and this is the framework of first-order approximations that may help the missile designer to better appreciate some of the concepts and issues involved. Specifically, the paper addresses the issue of figures of merit, *i.e.*, their validity and limitations for rating the TSR capability of IR dome materials, taking into consideration the special requirements associated with supersonic flight.

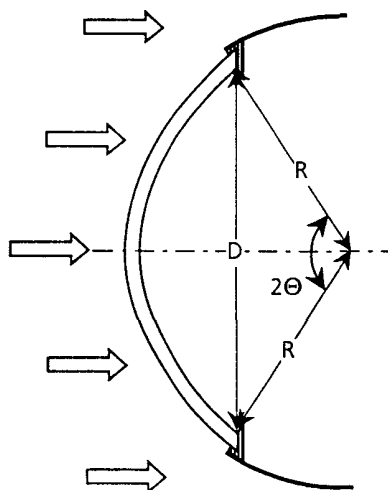


Fig. 1. *Hypothetical infrared missile dome configuration.*

Any viable missile dome structure (see Fig. 1) must be able to withstand the mechanical stresses induced by aerodynamic pressure as well as the thermal stresses induced by aerodynamic heating. In a supersonic flight environment, altitude and velocity determine the pressure load; in Sec. 2, I will use analytical formulas for assessing the impact of pressure differentials on required wall thicknesses, keeping in mind that the attachment design must be able to accommodate thermal

expansion mismatches over a broad temperature range. In a transient heating situation, the thermal response of the dome will be determined by the Biot number, and in Sec. 3, I take advantage of the model described in the Appendix for estimating the peak thermal stresses in a thermally thick and a thermally thin regime. In conjunction with fracture-strength related considerations, this should allow us to gain some insight on how to quantify the TSR capability (Sec. 4) and, in particular, to demonstrate that the widely accepted figure of merit R' has no theoretical justification. For the purpose of illustrating the discussion, I will focus in Sec. 5 on flight scenarios of current interest and examine how IR dome materials presently under consideration can be ranked in terms of their ability to survive the thermal shock on a "most severe" trajectory. Finally, the conclusions are stated in Sec. 6, and matters of a more tutorial nature are presented in Appendix.

2. Pressure Induced Stress

At Mach numbers $M_\infty \geq 3$, the pressure distribution on a spheroidal shell varies essentially as the cosine square of the station angle,⁷ which implies that, for worst-case type calculations, we may assume that the aerodynamic pressure on a truncated hemisphere is uniform and equal to the stagnation-point pressure p_{st} . In highly supersonic flight, a fully vented IR dome as in Fig. 1 must, therefore, be able to withstand a pressure load

$$\Delta p = p_{st} - p_\infty = p_\infty [(p_{st}/p_\infty) - 1] \quad , \quad (4)$$

where p_{st}/p_∞ refers to the pressure ratio across the aerodynamic shock and along the stagnation streamline:

$$\frac{p_{st}}{p_\infty} = \left[\left(\frac{\gamma+1}{2} \right) M_\infty^2 \right]^{\frac{\gamma}{\gamma-1}} \left[\left(\frac{2\gamma}{\gamma+1} \right) M_\infty^2 - \frac{\gamma-1}{\gamma+1} \right]^{\frac{-1}{\gamma-1}} \quad . \quad (5)$$

With γ set equal to 1.4, and free-stream pressures p_∞ that are representative of a U. S. Standard Atmosphere, the pressure differentials of interest here are as listed in Table 1 (see Sec. 5), which shows that the most severe pressure loads ($\Delta p \approx 200$ psi) occur at medium altitudes.

Such external pressures give rise to a complex stress pattern that reflects the nature of the edge attachment, *i.e.*, the stiffness of the dome interface with the support ring. For our purposes, it should be sufficient to consider the two limiting cases of (a) the simply supported shell that is free to bend when submitted to the action of a uniform normal pressure, and (b) the shell with built-in (or clamped) edges that is restrained from moving in the "radial" direction. For simply supported shells, the maximum stress induced by bending, σ_{max} , is tensile and obeys the equation⁸

$$\frac{\sigma_{max}}{\Delta p} = \frac{R}{2L} \left\{ \left[1.6 + 2.44 \sqrt{\frac{R}{L}} \sin(\theta) \right] \cos(\theta) - 1 \right\} \quad , \quad (6)$$

provided the dome aspect ratio, L/R , satisfies the condition

$$\frac{\sin^2(\theta)}{12} \leq \frac{L}{R} \leq \frac{\sin^2(\theta)}{1.2} \quad , \quad (7)$$

where θ designates the hemisphere truncation angle (see Fig. 1). For edge-constrained shells, the predominant stress should be compressive and localized at the base of the dome, near the interface; it is independent of truncation and relates to the aspect ratio in a very simple manner.⁸

$$\frac{\sigma_{\max}}{\Delta p} = -1.2 \frac{R}{L} \quad (8)$$

if the condition

$$\frac{\sin^2(\theta)}{12} \leq \frac{L}{R} \leq \frac{\sin^2(\theta)}{3} \quad (9)$$

holds. In Fig. 2, I display the results of evaluating Eq. (6) for angles θ ranging from 30 to 60 deg. which show that, on a relative scale, the bending stress depends solely on the wall thickness (the stress increases as the thickness decreases) and can be approximated by means of the relation

$$\frac{\sigma_{\max}}{\Delta p} \approx 0.581 \left(\frac{L}{R} \right)^{-3/2} \quad (10)$$

as long as the conditions (7) are satisfied. It is also seen that this stress represents a worst case in the sense that constraining the edge displacement would mitigate the stresses, especially for low-aspect-ratio domes.

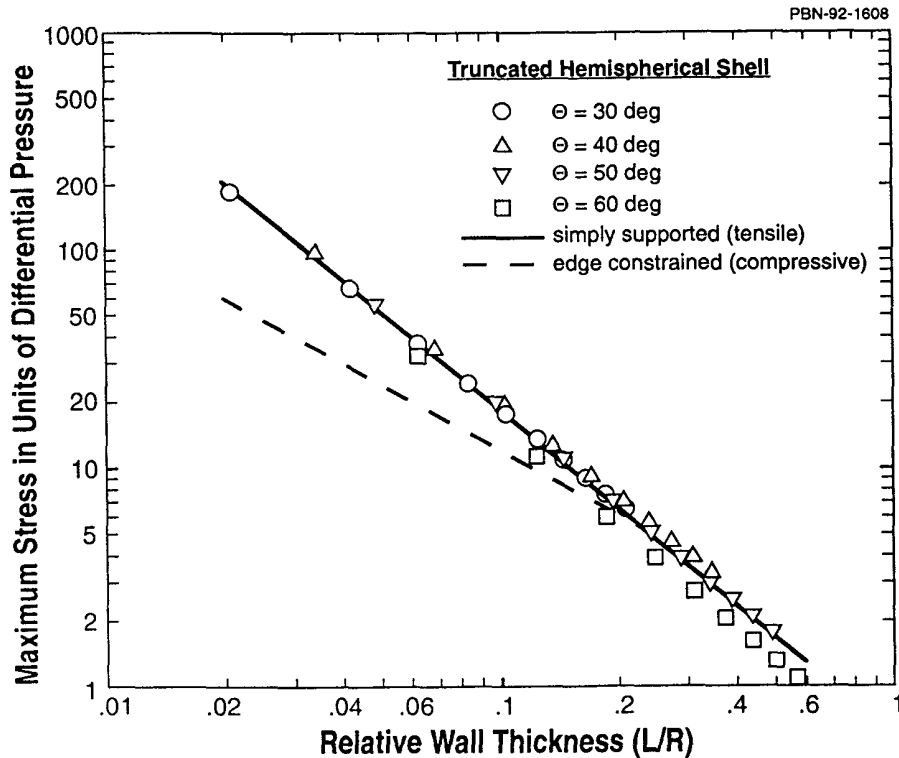


Fig. 2. Pressure-induced stress as a function of wall thickness, in relative units. The "data points" are bending stresses derived from Eq. (6), the angle θ referring to the truncation angle (see Fig. 1). The solid line illustrates the stress dependence for simply supported shells; the broken line is for edge-constrained shells as per Eq. (8).

At this point, I may reemphasize that the thickness of the dome plays a critical role not only in terms of thermal shock resistance (see Sec. 4) but also in the context of systems related considerations that are outside the purview of the present paper. Because of the thermal expansion mismatch at the interface of the infrared dome and its support structure, it is generally accepted

that a "floating" attachment scheme that decouples the dome from the missile body would be desirable,⁹ and such optimized attachment should result in pressure-induced tensile stresses as given by Eq.(10). The maximum tensile stress failure criterion, *i.e.* ,

$$\sigma_{\max} \leq \sigma_f / SF , \quad (11)$$

where σ_f refers to the nominal flexure strength of the dome material, and SF is an appropriate safety factor, then yields the minimum thickness required to prevent fracture. Since currently available IR transmitting dome materials are brittle ceramics, they may exhibit a wide range of fracture probabilities under apparently identical loadings, which suggests safety factors of at least four (4) if σ_f is the characteristic flexural strength derived from a Weibull statistical analysis. In this light, we conclude that the dome thickness required for withstanding a pressure load Δp with good probability of survival can be obtained from the following equation:

$$\frac{L_{\min}}{R} \approx 1.75 \left(\frac{\Delta p}{\sigma_f} \right)^{2/3} . \quad (12)$$

Note that the minimum thickness scales as $\sigma_f^{-2/3}$, which points to a steeper dependence on strength than for flat windows ($L_{\min} \propto \sigma_f^{-1/2}$).⁸

3. Thermally Induced Stress

When a missile moves through the atmosphere at supersonic velocities, the net effect of the formation of a shock wave, the compression in the stagnation region, and the energy dissipation by internal friction is to cover the wall of the missile "nose" with a layer of hot air called the boundary layer. There will be a transfer of heat between the boundary layer and the wall surface, but in the absence of heat losses through radiation or conduction, the wall always tends to assume an equilibrium temperature distribution that minimizes the heat transfer. Since according to Newton's law the thermal flux through a unit area is proportional to the difference between the actual wall temperature T_w and the adiabatic wall temperature (or recovery) temperature T_r , we may express the rate of convective heat flow as follows¹⁰:

$$q = h(T_r - T_w) , \quad (13)$$

where h represents the heat-transfer coefficient. The local recovery temperature cannot exceed the stagnation temperature,⁷

$$T_{st} = T_{\infty} \left[1 + (\gamma - 1) M_{\infty}^2 / 2 \right] , \quad (14)$$

which implies that, in a steady-state situation, a missile dome may reach but cannot exceed temperatures as given by Eq.(14). On a hemispherical dome, the recovery temperatures are known to drop off with distance away from the stagnation point,¹¹ but by no more than a few percent in the Mach-number range of interest here, even at off-axis stations where turbulent flow conditions may prevail. At Mach numbers $M_{\infty} > 3$, these temperatures are quite high, as evidenced in Table 1, which raises issues that are not addressed in this paper, namely dome-material melting and degradation of the IR transmittance. Of immediate concern, however, are matters relating to the heat-transfer coefficient h because this coefficient enters the definition of the Biot number [see Eq.(3)] and, thus, plays an essential role in characterizing the transient thermal environment. On a hemispherical dome, the heat-transfer coefficient at the stagnation point can be estimated by means of a semi-empirical formula,¹²

$$h_{st}\sqrt{2R} \approx 1.7c_p\sqrt{\rho_\infty\mu_\infty a_\infty} M_\infty (1+0.2M_\infty^2)^{0.1}, \quad (15)$$

which yields "numbers" as displayed in Fig. 3. for missile flight trajectories at altitudes up to 30 km and speeds ranging from Mach 1 to Mach 6; note that h_{st} scales as $1/\sqrt{R}$, which means higher heating rates for sharper nose tips. In principle, Eq. (15) holds only for the stagnation region since convective heat-transfer coefficients at off-axis stations strongly depend on local conditions, especially if the boundary layer turns turbulent beyond some distance x about the hemisphere in which case the heating rates are likely to be more severe than predicted by laminar flow theory.¹¹

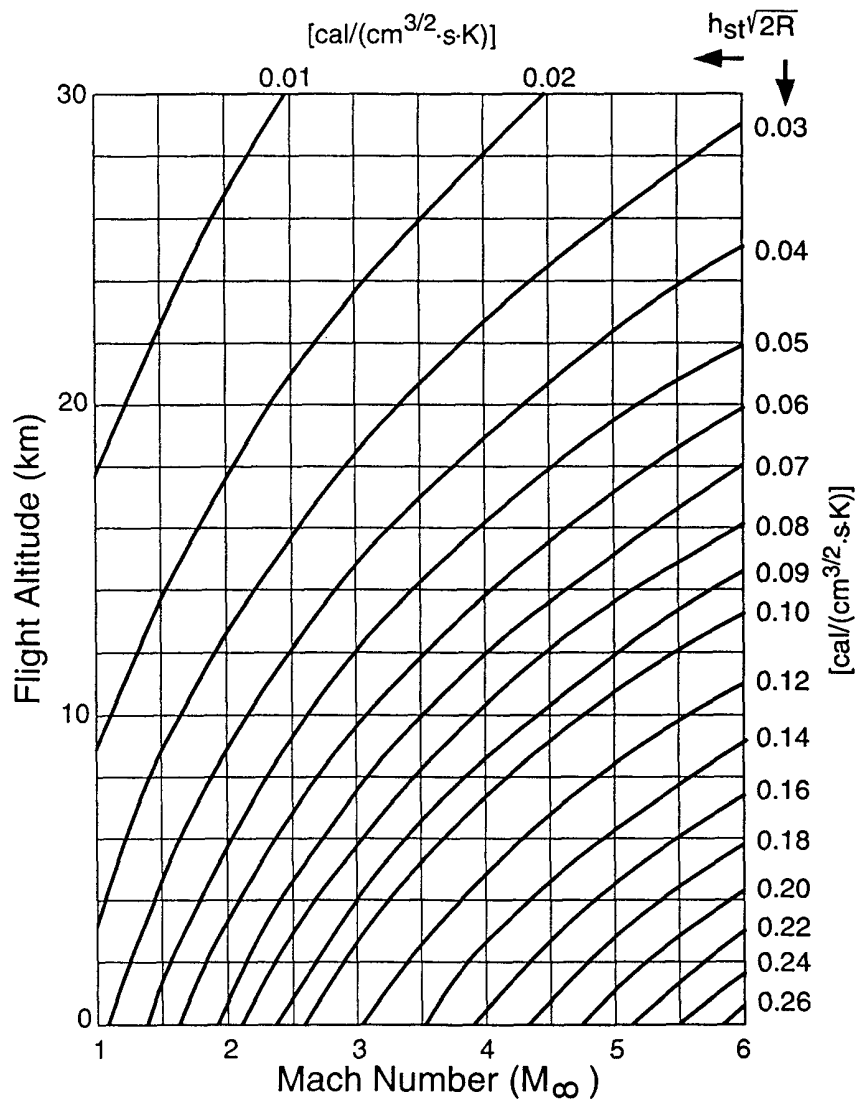


Fig. 3. Stagnation-point heat transfer nomogram for hemispherical missile domes of radius R ; the lines are $iso-h_{st}\sqrt{2R}$ contours obtained from Eq. (15).

Returning now to the stress problem, intuition tells us that, if the dome is housed in a compliant mount, aerodynamic heating will tend to produce tensile stresses on the inner (cold) surface of the dome and compressive stresses on the outer (hot) surface. In effect, the maximum

tensile stress should be given by an expression such as

$$\sigma_{\max} = (1/\text{TSF}) \alpha E' \Delta T, \quad (16)$$

where α is the thermal expansion coefficient, E' is the biaxial elastic modulus [$E' = E/(1-\nu)$], and ΔT is the temperature differential acting across the dome wall. The thermal stress factor (TSF) then would depend on the dome geometry, the attachment design, and above all, the transverse or axial temperature profile; for example, in the case of a complete spherical shell that is free to expand and has a linear temperature variation across the thickness, the thermal stress factor should be set equal to two (TSF=2).⁸ As demonstrated elsewhere (see the Appendix), in the initial transient phase, ΔT increases quite rapidly with time but depends upon the heat-flow pattern, which is controlled by the Biot number. Specifically, for *thermally thick domes*, the surface temperature may reach the recovery-temperature limit before the thermal front approaches the inner dome surface, which translates into

$$(\Delta T)_p \approx T_{st} - T_{iw}, \quad \text{Bi} \geq 1 \quad (17a)$$

at the stagnation point. For *thermally thin domes*, however, the temperature gradient peaks just about when the back-surface temperature begins to rise, which occurs long before the front surface approaches the stagnation temperature and, thus, leads to

$$(\Delta T)_p \approx (T_{st} - T_{iw}) \times \text{Bi}, \quad \text{Bi} < 1 \quad (17b)$$

the symbol T_{iw} referring to the inner or initial wall temperature, that is, at the onset of the shock. In a first approximation, therefore, these temperature differentials generate peak stresses as given by Eq. (16):

$$(\sigma_{\max})_p \approx \begin{cases} \frac{1}{\text{TSF}} \times \frac{\alpha E}{1-\nu} \times (T_{st} - T_{iw}) & \text{if } \text{Bi} \geq 1 \end{cases} \quad (18a)$$

$$\begin{cases} \frac{1}{\text{TSF}} \times \frac{\alpha E}{1-\nu} \times \text{Bi} \times (T_{st} - T_{iw}) & \text{if } \text{Bi} < 1 \end{cases}, \quad (18b)$$

the Biot number now pertaining to stagnation-point conditions. In both regimes, it is the tensile stress at the inner surface that initiates brittle fracture, if and when $(\sigma_{\max})_p$ exceeds the tolerable stress intensity. Note that, for "thick" domes, the peak stress should be essentially independent of the geometry since the thermal stress factor is not expected to be very dependent upon thickness; for "thin" domes, on the contrary, the stresses are linearly dependent upon the L parameter, which indicates that decreasing the wall thickness will reduce the thermal stress and, therefore, enhance the dome's resistance to thermal shock.

4. Thermal Shock Resistance

The problem of assessing the thermal shock resistance of infrared missile domes boils down to estimating the probability of mechanical failure induced by transient stresses: as in classical failure analysis, this task requires precise information on peak tensile stresses [$(\sigma_{\max})_p$] and, in addition, an appropriate model for the allowable stress intensities (σ_{\lim}). For brittle materials of nominal (or characteristic) strength σ_f , we may assume that a safety factor of four as in Sec. 2, *i.e.*,

$$\sigma_{lim} = \sigma_f/4 \quad (19)$$

provides enough of a "margin." which suggests to characterize the ability of surviving the thermal shock simply in terms of the ratio $\sigma_{lim}/(\sigma_{max})_p$, or

$$\frac{\sigma_{lim}}{(\sigma_{max})_p} = \begin{cases} \frac{TSF}{4} \times \frac{\sigma_f(1-\nu)}{\alpha E} \times \frac{1}{T_{st}-T_{iw}} & \text{if } Bi \geq 1 \quad (20a) \\ \frac{TSF}{4} \times \frac{\sigma_f(1-\nu)}{\alpha E} \times \frac{1}{Bi} \times \frac{1}{T_{st}-T_{iw}} & \text{if } Bi < 1 \quad (20b) \end{cases}$$

At this point, and following Kingery,⁴ we may set the stress ratio equal to one (1) and solve Eq.(20) for the allowable recovery temperature rise above the initial wall temperature:

$$(T_{st}-T_{iw})_{lim} = \begin{cases} \frac{TSF}{4} \times \frac{\sigma_f(1-\nu)}{\alpha E} & \text{if } Bi \geq 1, \quad (21a) \\ \frac{TSF}{4} \times \frac{\sigma_f(1-\nu)}{\alpha E} \times \frac{1}{Bi} & \text{if } Bi < 1. \quad (21b) \end{cases}$$

This procedure yields a direct measure of the TSR capability in the sense that it provides a compact expression for the allowable stagnation temperature rise; for convenience, we shall adopt the terminology of Palmer¹³ and refer to $(T_{st}-T_{iw})_{lim}$ simply as the "thermal shock temperature." This temperature thus reflects the range of rapid acceleration, or Mach number variation, that an IR dome can tolerate without undue risk of catastrophic failure. Evidently, the thermal shock temperature depends not only upon intrinsic material properties but also on the heat-flow pattern (thermally thick or thermally thin) as defined by the Biot number for stagnation-point conditions.

The thickness of the dome plays a critical role for two reasons: (a) It may have an impact on the heat-flow regime through the Biot number, and (b), in a thermally thin regime, the TSR performance will be enhanced by making the dome as thin as possible. In conjunction with the need to minimize the dome self-emission,¹ this points to "optimum" dome thicknesses, $L=L_{min}$, that are determined by aerostructural requirements as formulated in Sec. 2. Furthermore, since the heat-transfer coefficient at the stagnation point varies inversely as the square root of the dome radius [see Eq.(15)], in other words, since $h_{st}=h'_{st}/\sqrt{R}$ if h'_{st} refers to a 1-cm radius dome, it follows that, in the context of assessing the "ultimate" TSR of an IR dome, the Biot number should be expressed in a manner such as

$$Bi^* = 1.75 \times h'_{st} (\Delta p)^{2/3} \times \sqrt{R} / (k \sigma_f^{2/3}) \quad (22)$$

This expression, which holds for a minimum-thickness dome compatible with an external pressure load Δp , consists of a dimensionless constant times the product of two factors: $h'_{st}(\Delta p)^{2/3}$ and $\sqrt{R}/(k \sigma_f^{2/3})$. The first factor involves the Mach number and the flight altitude, exclusively [see Eqs.(5) and (15)], hence reflects the severity of the aero environment. The second factor involves the dome radius in addition to key material properties (thermal conductivity and fracture strength): note that Bi^* scales as \sqrt{R} , which emphasizes that high-fineness-ratio nose shapes are preferable not only for achieving low drag but also for enhancing the TSR, albeit this may conflict with

considerations relating to optical resolution since apertures $D=2R\sin(\theta)$ of at least 2.5 cm are required in the infrared.¹⁴

Returning now to Eq.(21), and upon inserting the Biot number expression for thickness-optimized hemispherical domes [Eq.(22)], it is seen that the TSR performance as measured in terms of thermal shock temperatures,

$$(T_{st}-T_{iw})_{lim}^* = \begin{cases} \frac{TSF}{4} \times \frac{\sigma_f (1-\nu)}{\alpha E} & \text{if } Bi^* \geq 1 \quad (23a) \\ \frac{TSF}{4} \times \frac{\sigma_f^{5/3} (1-\nu) k}{\alpha E} \times \frac{1}{1.75 h'_{st} (\Delta p)^{2/3} \sqrt{R}} & \text{if } Bi^* < 1, \quad (23b) \end{cases}$$

depends on specific material property combinations in addition to the radius of the dome and the aerodynamic/aerothermal load. Furthermore, it is important to bear in mind that the thermal stress factor TSF (see Sec. 3) depends on the dome configuration and, more importantly, the shape of the temperature distribution under peak stress conditions, which, in turn, involves the thermal diffusivity. If, for the sake of the argument, we choose to ignore the potential impact of thermal property variations on this factor, we find that, in a thermally thick regime, the TSR capability will be essentially controlled by the material figure of merit

$$FOM = \frac{\sigma_f (1-\nu)}{\alpha E}, \quad Bi^* \geq 1, \quad (24a)$$

which replicates the Hasselman parameter R for high rates of convective heating [see Eq.(1)]. In a thermally thin regime, however, the appropriate figure of merit should be

$$FOM = \frac{\sigma_f^{5/3} (1-\nu) k}{\alpha E}, \quad Bi^* < 1, \quad (24b)$$

which indeed includes the thermal conductivity just as the Hasselman parameter R' for low rates of heat convection [see Eq.(2)] but "weighs" the fracture strength more heavily because of the role of σ_f in fixing the dome thickness. Obviously, the material property combinations that affect the thermal shock resistance differ depending on the situation with regard to the Biot number (thermally thick or thermally thin); for identical materials under different loading conditions, or different materials under similar loadings, the relevant FoM may not be the same, which *de facto* negates the concept of a materials figure of merit for thermal shock. Nevertheless, and especially since the factor TSF should not be a strong function of material parameters, we may reasonably expect that figures of merit as proposed here can provide some guidance in selecting IR transmitting materials for missile-dome applications.¹⁵

5. Ranking the Candidates

For the purpose of illustrating the preceding considerations, I propose to evaluate and rank the TSR performance of candidate IR dome materials from the viewpoint of U. S. Air Force requirements for future generation air-to-air missiles. As currently envisioned,¹⁴ these requirements cover the range of altitudes and speeds delineated in Table 1, lines 1 to 3; the three scenarios refer to "low," "medium," and "high" altitudes of operation with contemplated peak

Table 1. *Air-to-air missile flight scenarios and relevant key numbers*

| SCENARIO | LOW ^(a) | MEDIUM ^(a) | HIGH ^(a) |
|--|----------------------|-----------------------|----------------------|
| Flight altitude (km) | 1 | 3 | 30 |
| Mach number at launch | 1 | 1.5 | 2 |
| Mach number at speed | 3 | 4 | 6 |
| Free-stream pressure (psi) | 13.0 ^(b) | 10.2 ^(b) | 0.174 ^(b) |
| Stagnation pressure ratio | 12.0 | 20.9 | 46.5 |
| Pressure differential (psi) | 143 | 203 | 7.91 |
| Free-stream temperature (K) | 282 ^(b) | 267 ^(b) | 227 ^(b) |
| Stagnation temperature (K) | 790 | 1121 | 1861 |
| Heat-transfer coefficient ($\text{Wcm}^{-2}\text{K}^{-1}$) | 0.324 ^(c) | 0.414 ^(c) | 0.081 ^(c) |

^a See Ref. 14.

^b Assumes a U. S. Standard Atmosphere.

^c For a 1-cm radius dome.

Table 2. *Infrared missile dome material candidates and key properties^a*

| Material candidate | Flexural strength (MPa) | Young's modulus (GPa) | Poisson's ratio | Thermal conductivity $\text{W}/(\text{m} \cdot \text{K})$ | Thermal exp. coeff. (10^{-6}K^{-1}) |
|-------------------------|-------------------------|-----------------------|-----------------|---|--|
| Al_2O_3 | 500 | 400 | 0.27 | 24 | 7 |
| ALON | 300 | 317 | 0.24 | 13 | 7 |
| diamond | ~2000 | 1050 | 0.16 | 2000 | 1 |
| GaAs | 60 | 86 | 0.31 | 53 | 6 |
| GaP | 100 | 103 | 0.31 | 97 | 6 |
| MgF_2 | 100 | 115 | 0.30 | 12 | 10 |
| spinel | 180 | 280 | 0.26 | 15 | 7 |
| Y_2O_3 | 150 | 170 | 0.30 | 14 | 7 |
| ZnS | 100 | 74 | 0.29 | 17 | 7 |
| ZnSe | 50 | 71 | 0.21 | 13 | 8 |

^a From Ref. 17.

Mach numbers of 3, 4, and 6, respectively, thus giving rise to a broad spectrum of aerodynamic/aerothermal loads that must be negotiated by an IR dome located in the missile nose section. Pressure differentials and recovery temperatures listed in Table 1 are as given by Eqs.(4) and (14), on assuming U. S. Standard Atmosphere free-stream pressures and temperatures.¹⁶ Note that even if the surface of the dome does not quite reach stagnation conditions because of the dome's radiant emittance for instance, the steady-state temperature at medium or high altitudes will exceed the working limits of most IR transmissive materials; as pointed out earlier, we are deliberately ignoring that aspect of the missile-dome problem. The heat-transfer coefficients listed in Table 1 also refer to the stagnation point and are as derived from Fig. 3 on setting the dome radius equal to 1 cm; it is seen that high-speed flight at medium altitude creates the most severe transient heating environment. Since this situation also holds with regard to pressure loads, we conclude that the medium-altitude scenario will be the most stressing though it does not encompass the highest temperatures.

Table 2 presents a listing of materials that are currently under consideration as potential dome materials for heat-seeking missiles.¹⁷ These materials are at different stages of development and show promise in terms of being capable of operating in severe thermal environments, but it is recognized that few of the candidates will be able to function as domes or windows in the Mach number range of interest here. Our objective is simply to rank these candidates from the point of view of their capability to withstand the thermal shock on a hypothetical most severe trajectory and to examine how figures of merit correlate with thermal shock temperatures. The properties that directly affect the thermal shock resistance (see Sec. 4) are also listed in Table 2; these are room-temperature data compiled by Harris¹⁷ that are believed to be quite adequate for our purposes. It will be recalled, however, that the fracture strength of optical ceramics is a "very extrinsic property"² in the sense that it depends on micro-structural features as well as the finish and the size of the test specimen; since the tabulation in Ref. 17 provides no relevant information, I take it that the strength values are indicative of characteristic strengths, σ_f , as specified earlier. An evaluation of the TSR capability then involves three computational tasks (minimum dome thickness, convection Biot number, thermal shock temperature), and I will briefly discuss each step in the next three paragraphs.

At Mach 4 on a medium-altitude trajectory, the pressure load amounts to 203 psi=1.40 MPa, which implies [see Eq.(12)] minimum dome thicknesses that obey the relation

$$L_{\min}/R = 2.19/\sigma_f^{2/3} \quad (25)$$

if σ_f is in megapascals; for the materials listed in Table 2, this yields relative thicknesses as indicated in Fig. 4. In this connection, it will be recalled that Eq.(25) only holds if the conditions (7) are satisfied, and Fig. 4 demonstrates that this is indeed the case for all the candidates but diamond as long as the hemisphere truncation angle θ exceeds 30 deg. With regard to diamond, I may point out that a flexural strength value of approximately 2 GPa as given in Table 2 probably overestimates the true strength of polycrystalline diamond since recent "ring-on-ring" measurements that were carried out on high-quality CVD material¹⁸ suggest $\sigma_f \approx 1$ GPa and, therefore, thicknesses that should be compatible with the stress model described in Sec. 2.

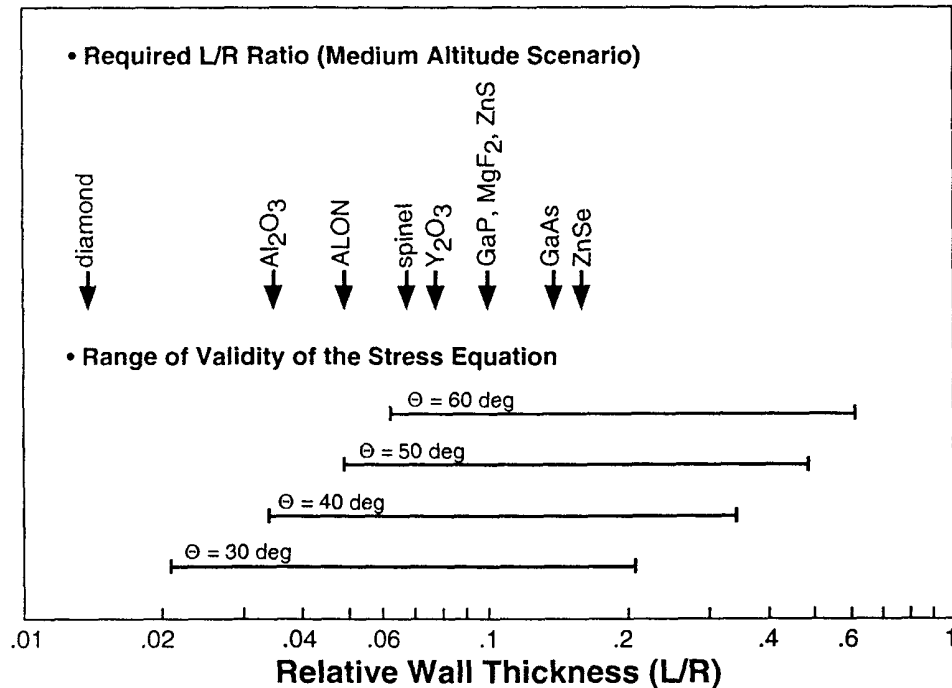


Fig. 4. Required dome thickness, on a most severe trajectory, in units of dome radius, for dome material candidates of current interest. Horizontal bars delineate the range of validity of the relevant stress model. The case of diamond is discussed in paragraph 3 of Sec. 5.

For minimum-thickness domes, a medium-altitude launch with "instantaneous" acceleration up to Mach 4, leads to Biot numbers that are best expressed as follows:

$$Bi^* = \frac{h'_{st} L_{min}}{\sqrt{R} k} = \frac{0.908 \sqrt{R}}{k \sigma_f^{2/3}}, \quad (26)$$

where R is in centimeters, k is in Watts per centimeter per degree Kelvin, and σ_f is in megapascals. Figure 5 displays the results of evaluating Eq.(26) for the ten candidate materials upon setting the dome radius equal to 2.5, 5, and 10 cm; it is immediately seen that, with the possible exception of domes made of ZnSe or MgF₂, the response to transient heating will be in the thermally thin mode. Of special interest is the case of diamond, which exhibits exceptionally low Biot numbers ($Bi^* < 0.001$) that minimize the temperature gradients across the thickness [see Eq.(17b)] and, by the same token, "explain" the unique TSR performance of this material.¹⁹

As defined in Sec. 4, the thermal shock temperatures (TST) depend on the stress factor TSF, which is not available for complex geometries such as missile domes but can be extracted, in principle, from the results of thermal shock testing that was carried out at NWC²⁰ and APL.²¹ Preliminary indications²² are that setting the factor TSF/4 equal to one (1) should be appropriate for ranking dome material candidates in terms of their TSR performance but not for drawing firm conclusions on allowable $T_{st} - T_{iw}$ temperatures, especially since the rate of convective heat transfer may peak at off-axis stations rather than the stagnation point (see Sec. 3). In this light, we may

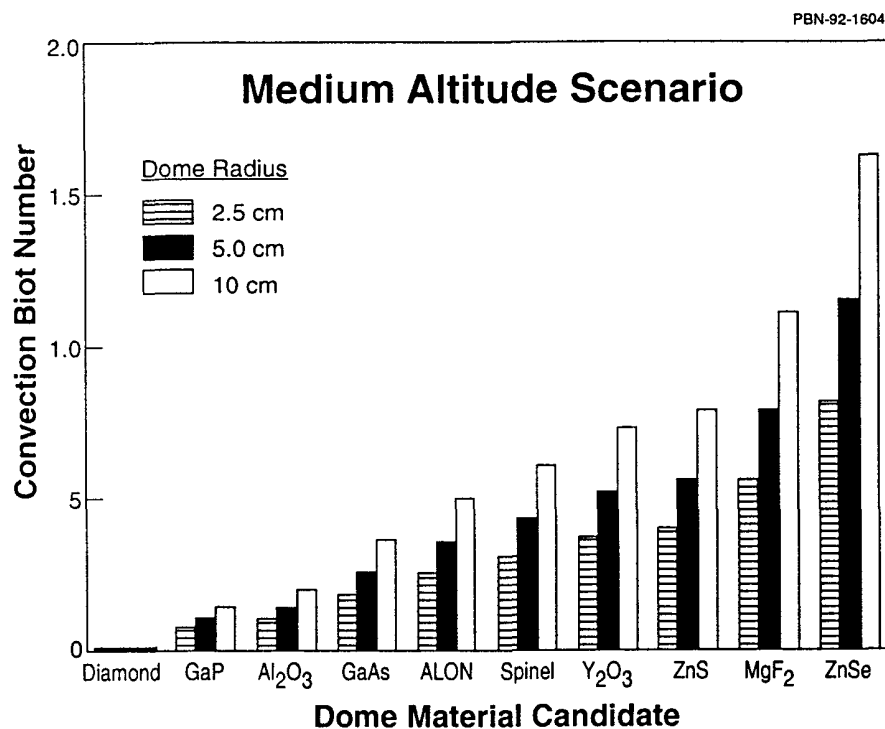


Fig. 5. Biot number of minimum-thickness missile domes on a most severe trajectory (medium altitude scenario).

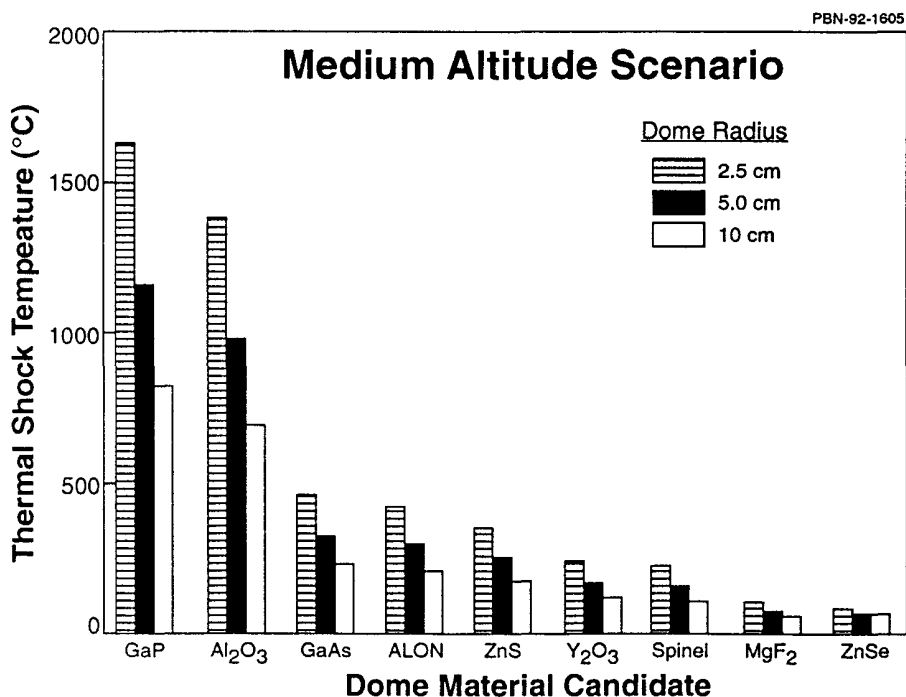


Fig. 6. Thermal shock temperature (TST) of minimum-thickness missile domes on a most severe trajectory (medium altitude scenario); note that the TST of diamond exceeds 10^6 °C and cannot be displayed on this chart.

rank the candidates simply on the basis of

$$\text{TST} = \begin{cases} \frac{\sigma_f (1-\nu)}{\alpha E} & \text{if } \text{Bi}^* \geq 1 \\ \frac{\sigma_f (1-\nu)}{\alpha E} \times \frac{1}{\text{Bi}^*} & \text{if } \text{Bi}^* < 1 \end{cases} \quad (27a)$$

with Bi^* as in Eq.(26), in other words, a Biot number that is representative of a most severe environment based on projected tactical missile requirements. On inserting the material property values listed in Table 2, this approach leads to the bar chart displayed in Fig. 6. (a) There are three obviously superior candidates (sapphire, GaP, and diamond), diamond providing the "ultimate" level of capability with $\text{TST} > 10^6$ K and, therefore, unsuitable for representation on a linear temperature scale as in Fig. 6. (b) The two thermally thick candidates (MgF_2 and ZnSe) exhibit mediocre TST figures and cannot be seriously considered for advanced applications. (c) Well-established materials such as GaAs, ALON, ZnS , Y_2O_3 , and spinel show surprisingly little variation in TSR capability, which renders it difficult to pass judgement on true relative performances in the absence of clear understanding regarding the impact of thermal diffusivities on the stress factor TSF.

Table 3. Thermal shock resistance ranking of IR dome material candidates

| Rank according to | TST ^(a) | TST ^(b) | R | R' | mod.R |
|--|-------------------------|-------------------------|-------------------------|-------------------------|-------------------------|
| 1 | diamond | diamond | diamond | diamond | diamond |
| 2 | GaP | GaP | ZnS | GaP | GaP |
| 3 | Al_2O_3 | Al_2O_3 | Al_2O_3 | GaAs | Al_2O_3 |
| 4 | GaAs | GaAs | GaP | Al_2O_3 | GaAs |
| 5 | ALON | ALON | ALON | ZnS | ALON |
| 6 | ZnS | ZnS | Y_2O_3 | ALON | ZnS |
| 7 | Y_2O_3 | Y_2O_3 | GaAs | Y_2O_3 | Y_2O_3 |
| 8 | spinel | spinel | ZnSe | spinel | spinel |
| 9 | MgF_2 | ZnSe | spinel | ZnSe | MgF_2 |
| 10 | ZnSe | MgF_2 | MgF_2 | MgF_2 | ZnSe |
| Correlation coefficient ^(c) : | | | 0.790 | 0.968 | 0.996 |

^a Medium-altitude scenario: The dome radius is 2.5 or 5 cm.

^b Medium-altitude scenario: The dome radius is 10 cm.

^c Of rankings based on figures of merit $R = \sigma_f(1-\nu)/\alpha E$, $R' = \sigma_f(1-\nu)k/\alpha E$, and $\text{mod.}R' = \sigma_f^{5/3}(1-\nu)k/\alpha E$ with rankings based on thermal shock temperatures (TST) as in Fig. 6.

Returning now to the figure-of-merit issue, it should be of interest to compare "true" rankings based on thermal shock temperatures as in Fig. 6 with rankings based on the two Hasselman

parameters [Eqs.(1) and (2)] and the modified figure of merit (mod.R') that was introduced in Sec. 4 for thermally thin domes. In Table 3, it is seen that diamond always ranks first, which is as expected since diamond, in effect, is not thermal stress limited. How the other dome material candidates rate depends on the "figure of merit" that has been selected, which substantiates our contention that the concept of a materials figure of merit for thermal shock has no real merit. In terms of correlation coefficients,²³ rankings based on mod.R' essentially replicate ($r^2=0.996$) the TST-derived "order of merit" but for MgF_2 and ZnSe , because material property combinations alone cannot take into account the transition from thermally thin to thermally thick that occurs as the domes get larger and thicker. The R parameter correlates rather poorly with TST-based rankings, which is not surprising considering that, even on a most severe trajectory, thermally thin conditions usually prevail (see Fig. 5). The R' parameter, however, ranks the candidates in a very acceptable manner ($r^2=0.968$), which is remarkable but perhaps fortuitous since R' has no theoretical justification (see Sec. 4); I may add that Compton's²⁴ finite element analysis of the transient thermal stress, combined with a fracture-statistical analysis of crack initiation through surface flaws, also points to trends in thermal shock failure that are consistent with "guidance" provided by the R' parameter.

6. Conclusion

© Since most of the materials that possess favorable optical properties in the infrared are relatively weak brittle solids, the problem of selecting dome materials for advanced IR-guided or dual-mode missiles requires a careful assessment of the dome's ability to withstand the thermal shock induced by transient heating on a fly-out trajectory. In this regard, it has become common practice to rely on simple figures of merit such as the Hasselman parameter R' for ranking the predicted performance of dome-material candidates. It was the purpose of this paper to demonstrate that the concept of a "universal" figure of merit for thermal shock has no merit since the ability of an IR dome to survive transient thermal stresses depends not only on intrinsic material properties but also on the thermal environment as defined by the Biot number.

© The thickness of the dome plays an essential role for two reasons: (a) It may have an impact on the heat-flow regime (thermally thick or thermally thin) through the Biot number, and (b), in a thermally thin regime, the TSR performance will be enhanced by making the dome as thin as possible. This points to optimum thicknesses, $L=L_{\min}$, that are determined by structural requirements as formulated in Sec. 2 and leads to the conclusion that, in the context of assessing the ultimate thermal shock resistance of an IR dome, the Biot number should be expressed as in Eq.(22). In addition to flight velocity and flight altitude, this expression involves three dome-related parameters: the thermal conductivity, the flexural strength, and the dome radius; since Bi^* scales as \sqrt{R} , it follows that smaller domes are preferable not only for achieving low drag but also for augmenting the resistance to thermal shock.

© The procedure outlined in Sec. 4 provides a direct measure of the TSR capability in the sense that it yields the "thermal shock temperature," i.e., the allowable recovery temperature rise above the wall temperature at the onset of the shock. For "thick" domes ($Bi \geq 1$), the thermal shock temperature should be essentially independent of the geometry and the environment since the thermal stress factor is not expected to be very dependent on dome parameters; for "thin" domes

($Bi^* < 1$), on the contrary, the performance depends not only on a specific material property combination (or figure of merit) but also on the radius of the dome and the aerodynamic/aerothermal load. In addition, the thermal stress factor may depend on the temperature profile and, hence, the thermal diffusivity, which will require further investigations if a precise evaluation of the TSR performance is desired.

© In a first approximation, or more specifically, on ignoring the potential impact of property variations on the stress factor TSF, the thermal shock resistance of a "thick" dome will be controlled by the material property combination $R = \sigma_f(1-\nu)/(\alpha E)$, which is precisely the Hasselman parameter for high rates of convective heating. In a thermally thin regime, however, the appropriate figure of merit should be $mod.R' = \sigma_f^{5/3}(1-\nu)k/(\alpha E)$, which includes the thermal conductivity in the same manner as the Hasselman parameter R' for low rates of heat transfer but puts more weight on the flexural strength because thinner domes are less vulnerable to thermally induced fracture. In this connection, I may emphasize that, from the point of view of generating a suitable data base, more effort must be devoted to obtaining reliable values for the *characteristic* strength of IR dome material candidates.

© On assuming that setting the stress factor equal to four ($TSF=4$) is indeed appropriate, we may rank IR dome material candidates simply on the basis of $TST=R$ if the condition $Bi \geq 1$ holds, and $TST=R/Bi$ if the condition $Bi < 1$ applies. This approach leads to the bar chart displayed in Fig. 6 and demonstrates that, in addition to diamond, which is the ultimate material in thermal shock resistance, there are two more candidates that exhibit clearly superior TSR capabilities, GaP and Al_2O_3 , but both are thermal stress limited to velocities of no more than Mach 5, on a medium-altitude trajectory. As expected, since thermally thin conditions usually prevail, the R parameter correlates rather poorly with TST-based rankings; the R' parameter, however, yields acceptable rankings, which is remarkable considering that there is no theoretical justification for using R' as a figure of merit.

Acknowledgement

I am indebted to R. Gentilman, formerly of Raytheon/Research, for stimulating my interest in problems relating to the phenomenology of thermal shock in IR missile domes.

Appendix

The initial transient temperature distribution generated by aerodynamic heating can be modeled in a particularly elegant manner, on using the "lumped parameter approximation" described in Ref. 1; here, I am taking advantage of this method to give the reader some insight into the underlying physical mechanisms that govern the thermal stress situation in missile domes. If ΔT represents the surface temperature increase ($\Delta T = T_s - T_i$), and ΔX is the effective thickness of the heated layer, both at time t subsequent to the onset of aerodynamic heating, we may write

$$h(T_r - T_i)t \approx \rho C_p \Delta T \times \Delta X \quad (A-1)$$

for the time-integrated heat flux per unit area, at any location, during the early phase of transient heating. Furthermore, on equating the rate of convective heat flow with the rate of conductive heat flow into the dome, it is seen that the relation

$$h(T_r - T_i) \approx k \Delta T / \Delta X \quad (\text{A-2})$$

applies. In effect, these two equations implicitly assume that the convection process operates across the heated layer. In combination, they yield

$$\Delta T \approx (T_r - T_i) \sqrt{t/t_{th}} \quad , \quad (\text{A-3})$$

where t_{th} is the thermal time constant,

$$t_{th} = \rho C_p k / h^2 \quad , \quad (\text{A-4})$$

that controls the surface temperature rise. Similarly, eliminating ΔT yields

$$\Delta X \approx L \sqrt{t/t_d} \quad , \quad (\text{A-5})$$

where t_d is the diffusion time constant,

$$t_d = \rho C_p L^2 / k \quad , \quad (\text{A-6})$$

which demonstrates that ΔX as well as ΔT increase as the square root of the elapsed time, but only for times t shorter than the two time constants. The ratio of the two constants, the time constant for the heat diffusion and the time constant for the temperature rise,

$$t_d/t_{th} = h^2 L^2 / k^2 = (Bi)^2 \quad , \quad (\text{A-7})$$

immediately tells us that it is the dimensionless Biot number, Bi , which incorporates the impact of aerodynamic heating rate, thickness of the dome, and its thermal conductivity, that best characterizes the transient heating process. For *thermally thick domes* ($Bi > 1$), we have $t_d > t_{th}$, which implies that the surface temperature rise ΔT may approach the $T_r - T_i$ limit at times t in the $t_{th} < t < t_d$ time "window," in other words, before the temperature of the back face begins to rise. For *thermally thin domes* ($Bi < 1$), on the contrary, the back face may get hot long before the front reaches the recovery temperature, which implies that, according to Eq. (A-3), the peak temperature difference should be

$$(\Delta T)_p \approx (T_r - T_i) \sqrt{t_d/t_{th}} = (T_r - T_i) \times Bi \quad , \quad (\text{A-8})$$

or less than for thermally thick domes. In summary, peak temperature gradients are expected to occur early during free flight, before or approximately at times comparable to the diffusion time; for our purposes, we may focus on stagnation-point conditions and set the peak temperature differentials as follows:

$$(\Delta T)_p \approx T_{st} - T_{iw} \quad , \quad Bi \geq 1 \quad (\text{A-9a})$$

$$(\Delta T)_p \approx (T_{st} - T_{iw}) \times Bi \quad , \quad Bi < 1 \quad (\text{A-9b})$$

where T_{st} refers to the recovery temperature at the stagnation point, T_{iw} is the inner wall temperature, *i.e.*, the wall temperature at the onset of the shock, and Bi designates the local Biot number ($Bi = h_{st} L / k$).

Glossary

| | | | |
|--------------|----------------------------------|--------------------|---------------------------------|
| a_{∞} | : sound velocity in air | T_r | : recovery temperature |
| Bi | : Biot number | T_w | : wall temperature |
| Bi^* | : Bi of minimum-thickness dome | T_{∞} | : free-stream temperature |
| c_p | : specific heat of air | T_{iw} | : initial wall temperature |
| E | : Young's modulus | T_{st} | : T_r at the stagnation point |
| E' | : biaxial modulus | T_{SF} | : thermal stress factor |
| FoM | : figure of merit | TST | : thermal shock temperature |
| h | : heat-transfer coefficient | α | : thermal expansion coefficient |
| h_{st} | : h at the stagnation point | γ | : specific heat ratio |
| h_{st}^* | : h_{st} of a 1-cm radius dome | Δp | : pressure differential |
| k | : thermal conductivity | ΔT | : temperature differential |
| L | : dome thickness | $(\Delta T)_p$ | : peak temperature differential |
| L_{min} | : minimum dome thickness | θ | : hemisphere truncation angle |
| M_{∞} | : Mach number | μ_{∞} | : viscosity of air |
| p_{st} | : stagnation-point pressure | ν | : Poisson's ratio |
| p_{∞} | : free-stream pressure | ρ_{∞} | : density of air |
| q | : heat flux rate | σ_f | : flexural strength |
| R | : dome radius | σ_{lim} | : allowable stress |
| R' | : Hasselman parameter | σ_{max} | : bending or thermal stress |
| SF | : safety factor | $(\sigma_{max})_p$ | : peak thermal stress |

References

1. F. McClintock, ed., "Mechanical Properties of Infrared Transmitting Materials." *Document No. NMAB-386* (National Academy of Sciences, Washington/DC, 1978), 293 pp.
2. R. Gentilman, "Current and Emerging Materials for 3-5 micron IR Transmission." *SPIE Proceedings*, vol. 683 (1986), pp. 2-11.
3. D. Hasselman, "Thermal Stress Resistance Parameters for Brittle Refractory Ceramics: A Compendium," *Ceramic Bulletin*, vol. 49 (1970), pp. 1033-7.
4. W. Kingery, "Factors Affecting Thermal Stress Resistance of Ceramic Materials." *Journal of The American Ceramic Society*, vol. 38 (1955), pp. 3-15.
5. W. Compton, "Application of Statistical Fracture Criteria to the Problem of Predicting Infrared Dome Thermal Shock Failures." *Document No. NWC-TP-6010* (Naval Weapons Center, China Lake/CA, 1978), 65 pp.
6. G. Wei, M. Pascucci, E. Trickett, S. Natansohn, and W. Rhodes, "Enhancement in Aerothermal Shock Survivability of Lanthana-Strengthened Yttria Windows and Domes." *SPIE Proceedings*, vol. 1326 (1990), pp. 33-47.
7. A. Shapiro, *The Dynamics and Thermodynamics of Compressible Fluid Flow* (The Ronald Press Co., New York/NY, 1953), vol. 1.
8. S. Timoshenko and S. Woinowsky-Krieger, *Theory of Plates and Shells* (McGraw-Hill Book Co., New York/NY, 1959), chap. 16.
9. C. Lee, "Evaluation of Several IR/RF Dome Configurations Subjected to High-Speed Flight Environments," *Proceedings of the Fourth DoD Electromagnetic Windows Symposium* (Office of Naval Technology, Arlington/VA, 1991), pp. 24-32.

10. L. Lorah and E. Rubin, "Aerodynamic Influences on Infrared System Design," in *The Infrared Handbook* (Office of Naval Research, Washington/DC, 1978), chap. 24.
11. I. Beckwith and J. Gallagher, "Heat Transfer and Recovery Temperatures on a Sphere with Laminar, Transitional, and Turbulent Boundary Layers at Mach Numbers of 2.00 and 4.15," *Document No. T.N.4125* (National Advisory Committee for Aeronautics, Washington/DC, 1957), 59 pp.
12. C. Klein, "Aerodynamic Heating of Hemispherical Irdomes of Supersonic Speeds," *Document No. T-844* (Raytheon Co., Waltham/MA, 1969), 30 pp.
13. J. Palmer, *High Power Laser Optics: A Study in Transient Heat Transfer* (Pro Se Publishing Co., San Diego/CA, 1990), chap. 9.
14. J. Rowe, A. Blume, and E. Boudreaux, "Dual-Mode Dome Requirements for Future Air-to-Air Missiles," *Proceedings of the Third DoD Electromagnetic Windows Symposium* (IIT Research Institute, Chicago/IL, 1989), pp. 79-95.
15. R. Schwartz, "The Navy Research Program on LWIR Dome Materials," *Proceedings of the Second DoD Electromagnetic Windows Symposium* (Arnold Engineering Development Center, Arnold AFS/TN, 1987), pp. 65-73.
16. M. Harris, "Meteorological Information," in *American Institute of Physics Handbook* (McGraw-Hill Book Co., New York/NY, 1972), chap. 2k.
17. D. Harris, "Powder Processing Technology for GaAs and GaP Infrared-Transmitting Materials," *Document No. NWC-TP-7145* (Naval Weapons Center, China Lake/CA, 1991), 24 pp.
18. K. Gray and G. Lu, "CVD Diamond as a Dual-Mode Dome Material," *Proceedings of the Fourth DoD Electromagnetic Windows Symposium* (Office of Naval Technology, Arlington/VA, 1991), pp. 262-8.
19. C. Klein, "Diamond Domes for High-Velocity Missiles: An Initial Assessment," *Proceedings of the Fourth DoD Electromagnetic Windows Symposium* (Office of Naval Technology, Arlington/VA, 1991), pp. 240-53.
20. F. Strobel, "Material Properties and Thermal Shock Performance for four IR Dome Materials," *Proceedings of the First DoD Electromagnetic Windows Symposium* (Naval Surface Weapons Center, Silver Spring/MD, 1985), pp. 431-8.
21. L. Weckesser, "Aerothermal Tests of IR Windows (U)," *Proceedings of the Third DoD Electromagnetic Windows Symposium* (IIT Research Institute, Chicago/IL, 1989), pp. 25-33 (CONFIDENTIAL).
22. C. Klein, "Thermal Shock Resistance of Infrared Missile Domes: Analysis and Testing," *in preparation*.
23. A. Anonymous, "Correlation Coefficient," in *Scientific Software Solutions: Decision Analysis* (Hewlett-Packard Co., Corvallis/OR, 1981), pp. 63-8.
24. W. Compton, "Aerothermal Shock Analysis of Yttria and Lanthana-Doped Yttria Seeker Domes," *Document No. NWC-TP-6994* (Naval Weapons Center, China Lake/CA, 1989), 93 pp.